

Comparison of IPMSM with distributed and concentrated windings

Soon-O Kwon, Sung-Il Kim, Jung-Pyo Hong

Abstract—Performance comparison of IPMSMs with distributed and concentrated windings is presented in this paper. Two IPMSMs are designed with identical rotor dimensions, air gap length, series turn number, stator outer radius, and axial length except winding configuration. Basic parameters and machine performance, such as inductances, resistances, back emf, output torque, and efficiency, are compared.

Index Terms—IPMSM, Concentrated windings, Distributed windings

I. INTRODUCTION

The application of IPMSM (Interior Permanent Magnet Synchronous Motor) is extending due to high power density and wide operating speed range with the help of reluctance torque and field weakening control. In order to maximize the advantage of its high power density, distributed windings is the reasonable choices for windings designs, because almost unit winding factor can be achieved. However, PM machines with distributed windings have several disadvantages such as difficulty in winding automation, long end windings, and larger copper loss than concentrated windings, etc. Comparing to distributed windings, concentrated windings enables easy windings automation and have short end windings, smaller copper loss, and require smaller space than distributed windings. However, winding factor of concentrated windings is generally smaller than distributed windings [1].

To improve output torque of PM machines with concentrated windings, many researches dealing with improving output torque of PM machines are undergoing. In design aspects, to improve the output torque, unequal tooth width of stator and appropriate choice of slot and pole number are introduced and the researches achieved improvement of output power of PM machines with concentrated windings or gives the direction in initial design stage [1-4]. However, the researches are concerned only with SPM motor with concentrated windings. Unlike to the SPM motors, inductances vary with rotor position

and current phase angle in IPMSM, and this variation have significant effects on motor performances.

The purpose of this paper is to study the effects on the characteristics of IPMSM when distributed winding is designed to concentrated windings. From basic parameter to output characteristics, both motors are closely compared. Initially, DIS (IPMSM with distributed windings) for high speed application is designed, then CON (IPMSM with concentrated windings) is designed with identical rotor part of DIS. From the basic motor parameters and characteristics, such as inductances, resistances, back emf, output torque, and efficiency, are compared.

II. ANALYSIS MODEL

A. Specifications and structure

Fig. 1 show the models studied in this paper. Both DIS and CON are designed for high speed application. (a) is distributed windings model with 4poles and 24slots and (b) is concentrated windings model with 4 poles and 6slots. The major geometric parameters of DIS and CON are identical; axial length, air gap length, rotor outer radius, stator outer radius, etc. and the only difference is the windings structure. Therefore, the effect of windings configuration on the motor performance can be easily observed.

Generally, concentrated windings machines have higher THD of back emf than distributed windings, therefore, CON is designed to have minimized THD of back emf by teeth tip and slot open width design.

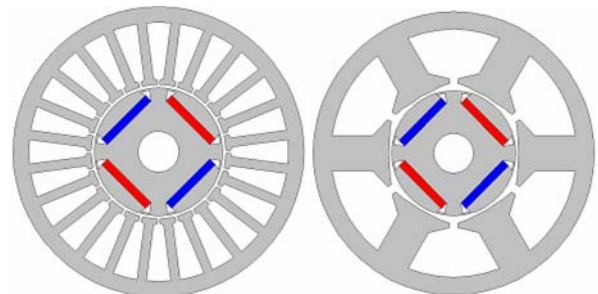


Fig. 1. Configuration of designed model

Fig. 2 shows the torque and power versus speed characteristics of both DIS and CON. Until 6,000rpm, constant torque of 17.5 Nm is maintained and from 6,000rpm to 20,000rpm, 11kW of output power is maintained. In the constant torque region, maximum torque per ampere control is considered and maximum efficiency control with field

Manuscript received July 15, 2006. This work was supported by grant No. RTI04-01-03 from the Regional Technology Innovation Program of the Ministry of Commerce, Industry and Energy (MOCIE).

Soon-O, Sung-Il Kim, Jung-Pyo Hong are with the Department of Electrical Engineering, Changwon National University, Changwon, Geongnam, Korea, 641-774 (phone: 82-55-262-5966; fax: 82-55-262-5965; e-mail: kso1975@changwon.ac.kr).

weakening is used in the constant power region.

Table I shows specification of the models. By redesigning windings configuration from distributed windings to concentrated windings, resistance of CON is lowered with lower current density. Lower current density could be achieved due to efficient filling factor of DIS.

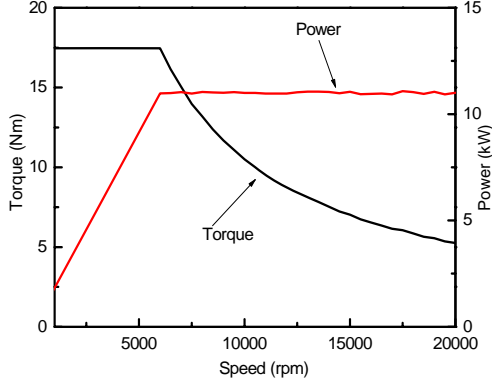


Fig. 2. Output Power characteristics

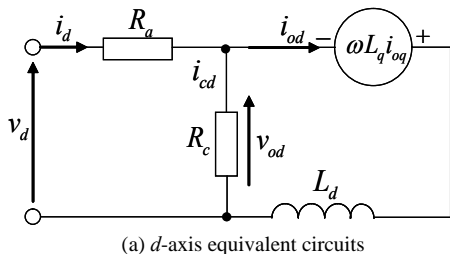
TABLE I. SPECIFICATION OF IPMSMS

	DIS	CON
Output power (kW)	11	11
Max. Torque (Nm)	17.5	17.5
Max. speed(rpm)	20,000	20,000
Number of poles/slots	4/24	4/6
Number of phases	3	3
Series turns	40	40
Number of coils	17	9
Number of parallel circuit	1	2
Resistance (mΩ)	45.7	37
Skew angle (°)	15	15

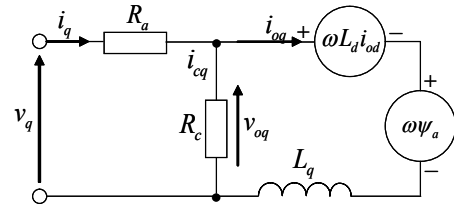
III. BASIC THEORY

A. *d-q* model of IPMSM

For the performance analysis of IPMSM, *d-q* model is generally used. Equivalent circuits for IPMSM based on a synchronous *d-q* model considering core losses are presented in Fig. 3. The mathematical model of the equivalent circuits is given by (1), (2), and (3) considering core loss [5]. By solving equations (1) ~ (3), characteristics of IPMSM is calculated in steady state in this paper.



(a) *d*-axis equivalent circuits



(b) *q*-axis equivalent circuits

Fig. 3. *d-q* equivalent circuit

$$\begin{bmatrix} v_d \\ v_q \end{bmatrix} = R_a \begin{bmatrix} i_{od} \\ i_{oq} \end{bmatrix} + \begin{pmatrix} 1 + \frac{R_a}{R_c} \\ \frac{R_a}{R_c} \end{pmatrix} \begin{bmatrix} v_{od} \\ v_{oq} \end{bmatrix} + P \begin{bmatrix} L_d & 0 \\ 0 & L_q \end{bmatrix} \begin{bmatrix} i_{od} \\ i_{oq} \end{bmatrix} \quad (1)$$

$$\begin{bmatrix} v_{od} \\ v_{oq} \end{bmatrix} = \begin{bmatrix} 0 & -\omega L_q \\ \omega L_d & 0 \end{bmatrix} \begin{bmatrix} i_{od} \\ i_{oq} \end{bmatrix} + \begin{bmatrix} 0 \\ \omega \Psi_a \end{bmatrix} \quad (2)$$

$$T = P_n \left\{ \Psi_a i_{od} + (L_d - L_q) i_{od} i_{oq} \right\} \quad (3)$$

where, i_d and i_q are *d*- and *q*-axis armature current, i_{cd} and i_{cq} are *d*- and *q*-axis iron loss current, v_d and v_q are *d*- and *q*-axis voltage, R_a is armature windings resistance per phase, R_c is iron loss resistance, Ψ_a is flux linkage by permanent magnet at no load, L_d and L_q are *d*- and *q*-axis armature self inductance, and P_n is pole pair.

B. Core loss calculation

Fig. 4 shows the procedure of core loss calculation using core loss data of magnetic material [5]. After calculating total iron loss, w_{total} , the core loss resistance R_c is calculated by (4).

$$R_c = v_o^2 / w_{total} \quad (4)$$

where, v_o is terminal voltage at no load and speed of core loss is calculated.

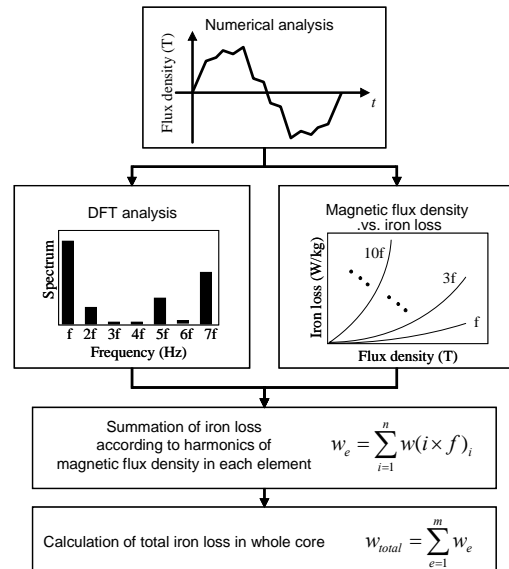


Fig. 4. Procedure of core loss calculation.

IV. COMPARISON OF CHARACTERISTICS

A. Comparison of basic characteristics

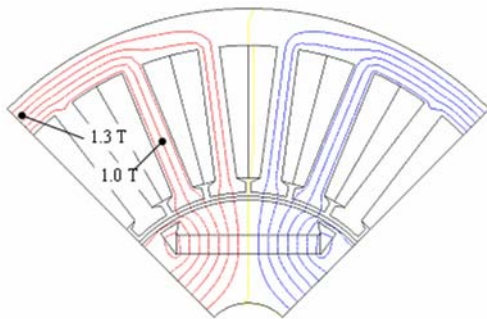
Flux distribution of DIS and CON at no load are compared in Fig. 5. CON shows lower flux density in the stator yoke than DIS, considering identical yoke thickness, that leads to smaller flux linkage of CON. Therefore, lower back emf and core loss of are produced.

No load back emfs are shown in Fig. 6. Due to pole/slot combination and windings configuration, CON shows 86.6 % of back emf to DIS having almost unit windings factor[1]. Due to skew effect and THD reduction design, both models show low THD.

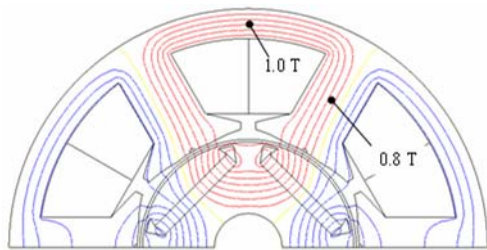
No load core losses are compared in Fig. 7. Due to lower THD of back emf and flux densities, CON shows lower core loss at entire speed region.

Generally, distributed windings with large slot numbers shows lower cogging torque than concentrated windings. In this study, CON designed to have minimum cogging torque within limitations, however it has still much higher cogging torque than DIS as shown in Fig. 8.

In Fig. 9, saliency ratio, L_d , and L_q are compared. To calculate L_d and L_q , 2D FEA is used. Flux linkages at no load, and each current and current phase angle are calculated. From the comparison, it is found that redesigning distributed windings to concentrated windings results in decrease of saliency ratio. Especially, the increase of L_d significantly affects to the decreased saliency ratio, while the effect of decreased L_q is small.



(a) Flux distribution in the yoke and teeth of DIS



(b) Flux distribution in the yoke and teeth of CON

Fig. 5. Flux density comparison

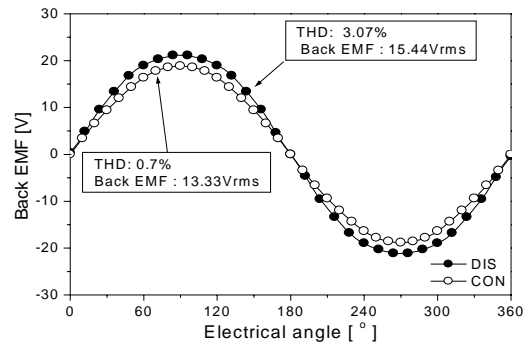


Fig. 6. Comparison of phase back emf and THD at 1000rpm

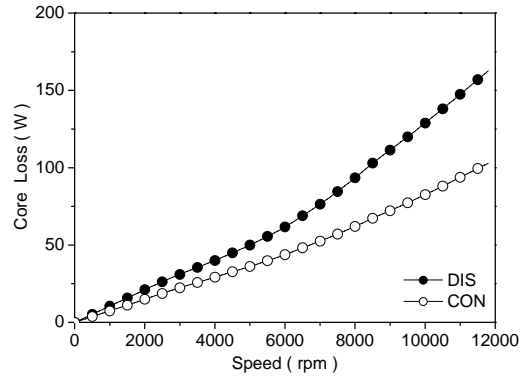


Fig. 7. Core loss comparison

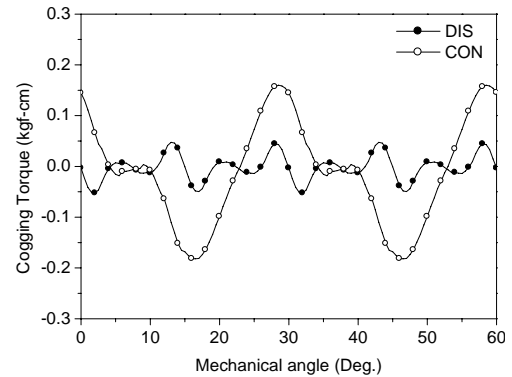
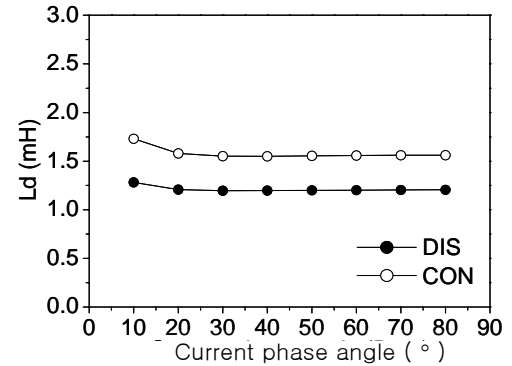
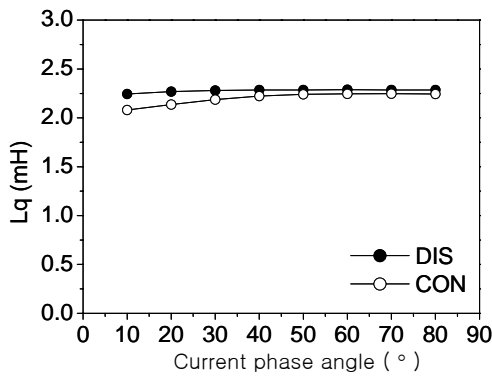


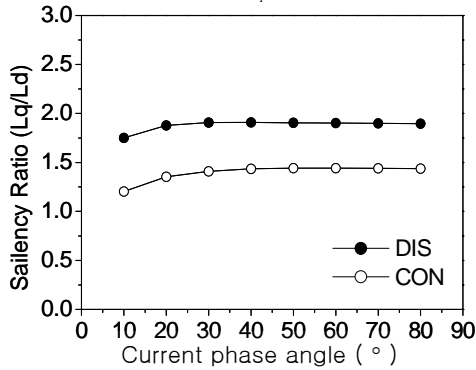
Fig. 8. Cogging torque comparison



(a) L_d



(b) L_q



(c) Saliency ratio

Fig. 9. Comparison of inductance and saliency ratio at rated current (43Arms)

B. Comparison of output characteristics

When both DIS and CON shows output powers shown in Fig. 2, other characteristics such as current, loss, line to line voltage, etc. are compared.

Fig. 10 shows current and voltage characteristics. Because CON has lower back emf and saliency ratio, it needs more current than DIS to produce required output torque in the constant torque region. However, when the back emf is saturated, CON requires less current due to smaller back emf to weaken.

Core loss and copper loss are shown in Fig. 11. It is found that currents of CON is higher in the constant torque region, however, copper loss becomes close to DIS, that is caused by lower phase resistance of CON.

Resultant efficiencies of both models are shown in Fig. 12. Due to low copper losses DIS shows higher efficiency in the constant torque region, but the difference is not significant. In the constant power region, due to low field weakening current, CON shows higher efficiency than DIS.

Output torque and ripples at 43Arms are calculated by 2D FEA and shown in Fig. 13, where maximum torque per ampere operation is considered. Due to lower back emf saliency ratio, CON shows lower output torque than DIS at identical input current. It is notable that maximum torque of CON is about 86.7% of DIS.

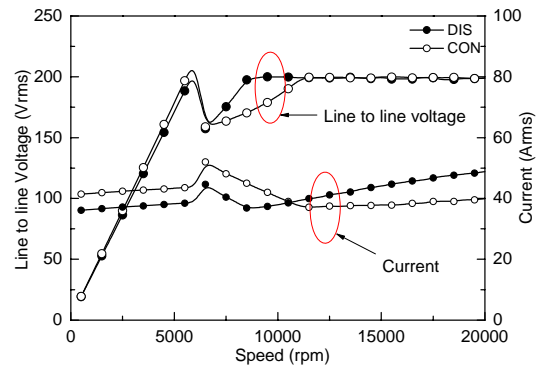


Fig. 10. Voltage and current comparison

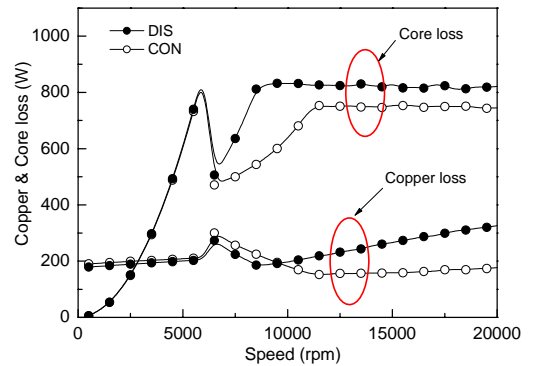


Fig. 11. Core loss and copper loss comparison

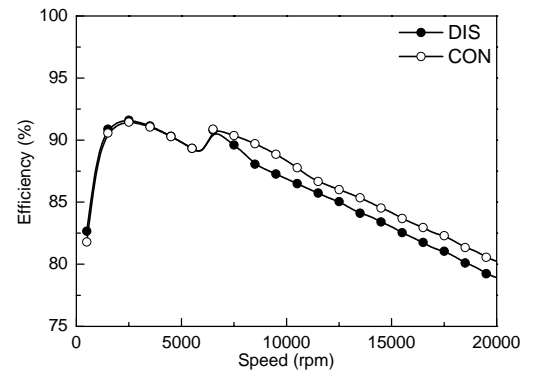


Fig. 12. Efficiency

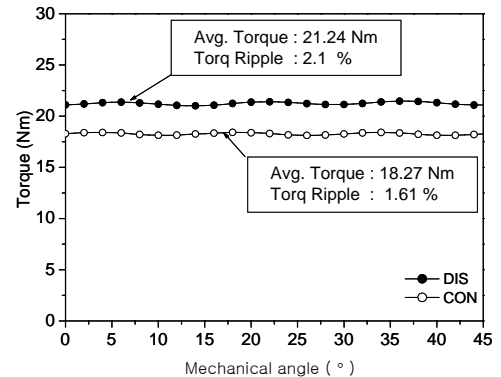


Fig. 13. Output torque and torque ripple at rated current

V. SUMMARY

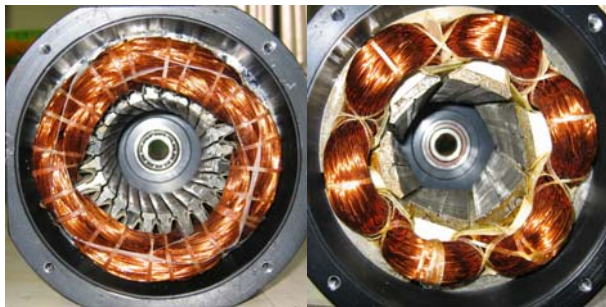
Characteristics of IPMSMs with distributed and concentrated windings are compared in this paper.

More current is required for concentrated windings than distributed windings model due to lower back emf and saliency ratio in constant torque region. The reason for more input current is that the decrease of magnetic torque and reluctance torque. Magnetic torque is reduced by decreased windings factor and the decrease of reluctance torque is caused mainly by increase of L_d .

In the constant power region, lower current is required for concentrated windings due to lower back emf to weaken and increased d-axis inductance.

Therefore, even though more current is required for concentrated windings in the constant torque region, copper loss is close to the distributed windings and less current with high efficiency is achieved in the field weakening region due to low back emf and higher d-axis inductance, and it is expected that concentrated windings is more suitable than distributed windings when field weakening operation at high speed is used.

Fig.14 shows the fabricated concentrated and distributed winding IPMSM. Fig. 15 shows back emf comparisons at 1000rpm of analysis and experimental results. Other characteristics of both motors will be verified in the next study.



(a) DIS (b) CON



(c) Rotor

Fig. 14. Fabricated DIS and CON model

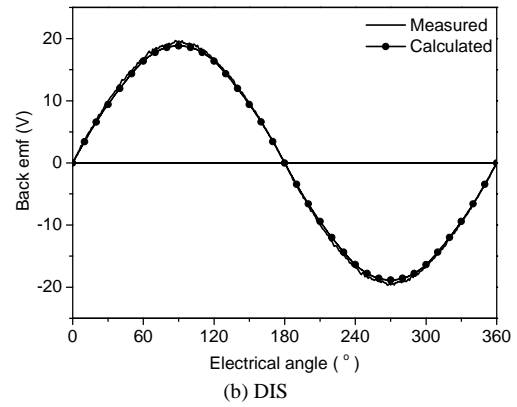
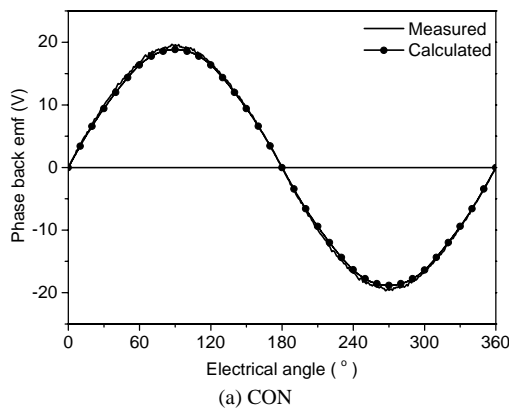


Fig. 15. Comparison of phase back emf with measurements (b) DIS

REFERENCES

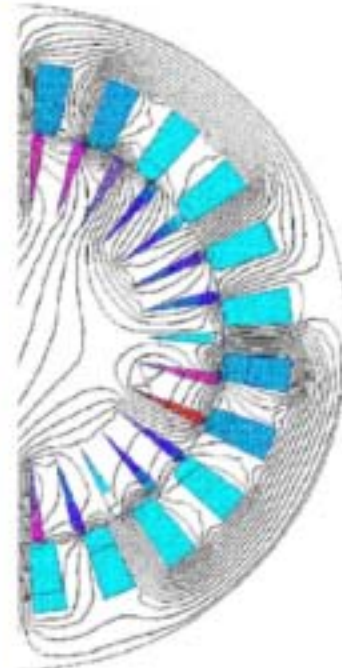
- [1] Freddy Magnussen, Chandur Sadarangani, "Winding Factors and Joule Losses of Permanent Magnet Machines with Concentrated Windings", IEEE Industry Applications Society Annual Meeting, Oct., 2004
- [2] D. Ishak, Z.Q. Zhu, D. Howe. " Permanent Magnet Brushless Machines with Unequal Tooth Widths and Similar Slot Pole Numbers ", IEEE Industry Applications Society Annual Meeting, Oct., 2004
- [3] Pia Salminen, Markku Niemelä and Juha Pyrhönen, Juhani Mantere, "Performance analysis of fractional slot wound Pm motors for low speed applications", IEEE Industry Applications Society Annual Meeting, Oct., 2004
- [4] Sung-Il Kim, Ji-Young Lee, Young-Kyoun Kim, Jung-Pyo Hong, Yoon Hur, Yeon-Hwan Jung, "Optimization for Reduction of Torque Ripple in Interior Permanent Magnet Motor by Using the Taguchi Method", IEEE Transactions on Magnetics, vol. 41, No. 5, May. 2005.
- [5] Ji-Young Lee, Sang-Ho Lee, Geun-Ho Lee, Jung-Pyo Hong, "Determination of Parameters considering Magnetic Nonlinearity in an Interior Permanent Magnet Synchronous Motor", IEEE Transactions on Magnetics, vol. 42, No. 5, April. 2006.



(a) CON

XVII International Conference on Electrical Machines

ICEM 2006



CONFERENCE PAPERS

Browse the ICEM 2006 Full Papers by:

- **Session**
- **Author**

September 2-5, 2006

Chania, Crete Island, Greece

Organising Institutions:



National
Technical
University of
Athens

Technical
University of
Crete

Aristotle
University of
Thessaloniki

University of
Patras

Democritus
University of
Thrace

15:30-16:40 POSTER (DIALOGUE) SESSION PSA1: PERMANENT MAGNET MACHINES

Saturday, September 2nd 2006

No	Ref	Paper title	Authors	Country of the corresponding author
PSA1-1	141	A Permanent Magnet Generator for Small Scale Wind Turbines	J.R. Bumby, N. Stannard and R. Martin	UK
PSA1-2	313	A Method for Dynamic Analysis of an Interior Permanent Magnet Motor Based on Nonlinear Magnetic Circuit	K. Nakamura, M. Ishihara, and O. Ichinokura	Japan
PSA1-3	163	High-speed permanent magnet generators design and testing	Yanush Danilevich, Victor Antipov	Russia
PSA1-4	180	An Attempt to Extend the Flux Weakening Range of a Single Stator Dual Rotor PM Machine	Imen Abdennadher, Ahmed Masmoudi and Ahmed Elantably	Tunisia
PSA1-5	234	Numerical design of DC brush motor with rare-earth magnets for ABS system including tolerances of input parameters	G. Ombach, J. Junak and A. Ackva	Germany
PSA1-6	244	A Stator Turn Fault Tolerant Strategy for Interior PM Synchronous Motor Drives in Safety Critical Applications	Youngkook Lee and T.G. Habetler	USA
PSA1-7	245	Comparative Evaluation of Axial Flux versus Radial Flux Permanent Magnet Synchronous Machines	M. Krishnamurthy, B. Fahimi and K. D. Oglesby	USA
PSA1-8	249	Design and Implementation of a Tubular Brushless DC Motor for Direct-Drive Applications	S.H. Mao, B.J. Lin, and M.C. Tsai	Taiwan
PSA1-9	250	Design of Interior Permanent Magnet Motors for Smoothing Back-EMF Waveform	H.S. Chen and M.C. Tsai	Taiwan
PSA1-10	251	Development of the Discontinuous Primary Permanent Magnet Linear Synchronous Motor	Kenji Suzuki, Yong-Jae Kim, Masaya Watada and Hideo Dohmeki	Japan
PSA1-11	254	Optimised design of concentrated winding PM brushless motors	A. Castagnini, P. Faure Ragani, G. Secondo	Italy
PSA1-12	266	Evaluation of Eddy Current Loss in Tubular Permanent Magnet Motors by Three-Dimensional Finite Element Analysis	J. Chai, J. Wang and D. Howe	UK
PSA1-13	267	Magnetic Field Distribution in Brushless Permanent Magnet AC Motors with Interior Permanent Magnets (IPM) and Slotted Stator	F. Poltschak, W.Amrhein	Austria
PSA1-14	274	A Brushless Permanent Magnet Motor with Hybrid Windings	M. C. Tsai and L. Y. Hsu	Taiwan
PSA1-15	276	Torque ripple reduction design of Multi-layer Interior Permanent Magnet Synchronous Motor by using Response Surface Methodology	Liang Fang, Soon-O Kwon, Peng Zhang, Jung-Pyo Hong	China
PSA1-16	311	Reluctance Network Analysis Model of a Permanent Magnet Generator Considering an Overhang Structure	K. Nakamura, M. Ishihara, and O. Ichinokura	Japan
PSA1-17	312	Multipolar Reluctance Generator Using Stator Core with Permanent Magnet	O. Ichinokura, T. Ono, T. Tashiro, K. Nakamura, and A. Takahashi	Japan
PSA1-18	346	Distribution, coil-span and winding factors for AFPM with concentrated windings	S. E. Skaar, Ø. Krøvel, R. Nilssen	Norway
PSA1-20	284	Application of a Toroidal Harmonic Expansion for Computing the Magnetic Field from a Balanced 6-Pole Permanent-Magnet Motor	J. Selvaggi, S. Salon, O. Kwon, and M.V.K. Chari	USA

11:40-13:20 ORAL SESSION OTM4: TESTING, MEASUREMENTS, ACOUSTIC NOISE AND VIBRATION ASPECTS

Tuesday, September 5th 2006

Ariadne Room

No	Ref	Paper title	Authors	Country of the corresponding author
OTM4-1	320	Testing of Electric Machines with a Dedicated System for Data Acquisition and Processing	Voicu Groza, Marius Biriescu, Vladimir Crețu, Gheorghe Liuba, Martián Mot , Gheorghe Madescu	Romania
OTM4-2	197	The increase of the magnetic noise of induction motors due to the low order excitation modes generated by the rotor eccentricity	S.L. Nau, R. Beck, H.L.V. dos Santos, N. Sadowski, R. Carlson	Brazil
OTM4-3	452	Monitoring of Induction Motors Rotor Faults by non invasive sensors	A. Bellini, C. Concari, G. Franceschini, C. Tassoni, A. Toscani	Italy
OTM4-4	505	Acoustic Noise and Displacement Analysis of a 3-phase Transformer Core Under Sinusoidal and PWM Excitations	X G Yao, Thant P P Phway, A J Moses, F Anayi	UK
OTM4-5	546	Optimal Design to reduce Acoustic Noise in Interior Permanent Magnet Motor using Response Surface Methodology	Sang-Ho Lee, Suk-Hee Lee, Jung-Pyo Hong, Sang-Moon Hwang, Ji-Young Lee, and Young-Kyoun Kim	Korea

15:30-16:40 POSTER (DIALOGUE) SESSION PSA1: PERMANENT MAGNET MACHINES

Saturday, September 2nd 2006

No	Ref	Paper title	Authors	Country of the corresponding author
PSA1-1	141	A Permanent Magnet Generator for Small Scale Wind Turbines	J.R. Bumby, N. Stannard and R. Martin	UK
PSA1-2	313	A Method for Dynamic Analysis of an Interior Permanent Magnet Motor Based on Nonlinear Magnetic Circuit	K. Nakamura, M. Ishihara, and O. Ichinokura	Japan
PSA1-3	163	High-speed permanent magnet generators design and testing	Yanush Danilevich, Victor Antipov	Russia
PSA1-4	180	An Attempt to Extend the Flux Weakening Range of a Single Stator Dual Rotor PM Machine	Imen Abdennadher, Ahmed Masmoudi and Ahmed Elantably	Tunisia
PSA1-5	234	Numerical design of DC brush motor with rare-earth magnets for ABS system including tolerances of input parameters	G. Ombach, J. Junak and A. Ackva	Germany
PSA1-6	244	A Stator Turn Fault Tolerant Strategy for Interior PM Synchronous Motor Drives in Safety Critical Applications	Youngkook Lee and T.G. Habetler	USA
PSA1-7	245	Comparative Evaluation of Axial Flux versus Radial Flux Permanent Magnet Synchronous Machines	M. Krishnamurthy, B. Fahimi and K. D. Oglesby	USA
PSA1-8	249	Design and Implementation of a Tubular Brushless DC Motor for Direct-Drive Applications	S.H. Mao, B.J. Lin, and M.C. Tsai	Taiwan
PSA1-9	250	Design of Interior Permanent Magnet Motors for Smoothing Back-EMF Waveform	H.S. Chen and M.C. Tsai	Taiwan
PSA1-10	251	Development of the Discontinuous Primary Permanent Magnet Linear Synchronous Motor	Kenji Suzuki, Yong-Jae Kim, Masaya Watada and Hideo Dohmeki	Japan
PSA1-11	254	Optimised design of concentrated winding PM brushless motors	A. Castagnini, P. Faure Ragani, G. Secondo	Italy
PSA1-12	266	Evaluation of Eddy Current Loss in Tubular Permanent Magnet Motors by Three-Dimensional Finite Element Analysis	J. Chai, J. Wang and D. Howe	UK
PSA1-13	267	Magnetic Field Distribution in Brushless Permanent Magnet AC Motors with Interior Permanent Magnets (IPM) and Slotted Stator	F. Poltschak, W.Amrhein	Austria
PSA1-14	274	A Brushless Permanent Magnet Motor with Hybrid Windings	M. C. Tsai and L. Y. Hsu	Taiwan
PSA1-15	276	Torque ripple reduction design of Multi-layer Interior Permanent Magnet Synchronous Motor by using Response Surface Methodology	Liang Fang, Soon-O Kwon, Peng Zhang, Jung-Pyo Hong	China
PSA1-16	311	Reluctance Network Analysis Model of a Permanent Magnet Generator Considering an Overhang Structure	K. Nakamura, M. Ishihara, and O. Ichinokura	Japan
PSA1-17	312	Multipolar Reluctance Generator Using Stator Core with Permanent Magnet	O. Ichinokura, T. Ono, T. Tashiro, K. Nakamura, and A. Takahashi	Japan
PSA1-18	346	Distribution, coil-span and winding factors for AFPM with concentrated windings	S. E. Skaar, Ø. Krøvel, R. Nilssen	Norway
PSA1-20	284	Application of a Toroidal Harmonic Expansion for Computing the Magnetic Field from a Balanced 6-Pole Permanent-Magnet Motor	J. Selvaggi, S. Salon, O. Kwon, and M.V.K. Chari	USA

10:20-11:30 POSTER (DIALOGUE) SESSION PTM2: DRIVES OF SYNCHRONOUS, PM AND DC MACHINES

Tuesday, September 5th 2006

No	Ref	Paper title	Authors	Country of the corresponding author
PTM2-1	526	Operational Behaviour of Industrial DC Drives in Paper Machines in Relation to Elastic Shafts Characteristics	C. Michael, A. Safacas	Greece
PTM2-3	344	Accurate Torque Control of VSI Fed Synchronous Machine Under Normal or Fault Conditions Using Discrete Modelling of Airgap Flux	M. Bekemans, F. Labrique, E. Matagne	Belgium
PTM2-4	702	Brushless, Self-Excited Synchronous Field-Winding Machine for Variable-Speed Drive Applications	Alexander Rovnan, Heath Hofmann	USA
PTM2-5	128	The New Methodology Of The Power Loss Calculation Under Deformed Flux Conditions	Z. Gmyrek, A. Boglietti, A. Cavagnino	Poland
PTM2-6	415	AC High Dynamometer for testing motor drive system	Gildong Kim, Hanmin Lee, Sehchan Oh, Sunghyuk Park, Changmu Lee	Korea
PTM2-7	341	Fast Prototyping of Vector Controllers for Interior PM Synchronous Motors	M. Tursini, A. Scotti, D. D'Antonio, and E. Chiricozzi	Italy
PTM2-8	379	Current Waveform Analysis of PWM Inverter-Fed Permanent Magnet Synchronous Machine Accounting for Cross-Magnetization	M. Kimura, K. Ide, H. Mikami	Japan
PTM2-9	342	Sensorless Control of PM Synchronous Motors with Luenberger Observer: Theoretical Issues and Implementation Results	M. Tursini, A. Scafati, R. Petrella	Italy
PTM2-10	460	Speed Control of Permanent Magnet Synchronous Motors by Current Vector Control	P. Fernandez, J. A. Goemes and A. M. Iraolagoitia	Spain
PTM2-11	626	Line-Start Permanent-Magnet Chemical Pump Drives	A.C. Smith and E.Peralta Sanchez	UK
PTM2-12	237	Versatile High Torque Direct Drive with PM-Excitation and Duplex Stator Arrangement	W.-R. Canders, H. Mosebach, M. R. Rezaei	Germany
PTM2-13	257	A Novel Drive Strategy for Vibration Suppression in Permanent Magnet Brushless DC Motor	Tao. Sun, Gen-Ho Lee, Jeng-Pyo Hong	Korea
PTM2-14	129	Implementation of an active converter for high quality dc drive performance	N.N. Barsoum, S.K. Wong	Malaysia
PTM2-15	155	Controlled DC Electric Drive Based on Stochastic Calculation Techniques	Achmad Alyan and Raul Rabinovici	Israel
PTM2-16	307	Determination of the Optimum Power Factor and Efficiency of a Characteristic DC Drive System via Simulation	K. Georgakakos, A. Safacas, I. Georgakopoulos	Greece
PTM2-17	440	Optimal Integral State Feedback controller for a DC motor	H. Delavari, GH. Alizadh, M. Sharifan,	Iran
PTM2-18	255	Simplified sensorless control technique for wound rotor synchronous motor	F. Chabour, J. P. Vilain, P. Macret, P. Masson, L. Kobylansky	France